Article

New Bounds for the Mass of Warm Dark Matter Particles Using Results from Fermionic King Model

Luisberis Velazquez

Departamento de Física, Universidad Católica del Norte, Av. Angamos 0610, Antofagasta 124000 , Chile; lvelazquez@ucn.cl

Abstract: After reviewing several aspects about the thermodynamics of self-gravitating systems that undergo the evaporation (escape) of their constituents, some recent results obtained in the framework of fermionic King model are applied here to the analysis of galactic halos considering warm dark matter (WDM) particles. According to the present approach, the reported structural parameters of dwarf galaxies are consistent with the existence of a WDM particle with mass in the keV scale. Assuming that the dwarf galaxy Willman 1 belongs to the region III of fermionic King model (whose gravothermal collapse is a continuous phase transition), one obtains the interval $1.2\,\text{keV} \le \text{m} \le 2.6\,\text{keV}$ for the mass of WDM particle. This analysis improves previous estimates by de Vega and co-workers [Astropart. Phys. 46 (2013) 14–22] considering both the quantum degeneration and the incidence of the constituents evaporation. This same analysis evidences that most of galaxies are massive enough to undergo a violent gravothermal collapse (a discontinuous microcanonical phase transition) that leads to the formation of a degenerate core of WDM particles. It is also suggested that quantum-relativistic processes governing the cores of large galaxies (e.g., the formation of supermassive black holes) are somehow related to the gravothermal collapse of the WDM degenerate cores when the total mass of these systems are comparable to the quantum-relativistic characteristic mass $M_c = (\hbar c/G)^{3/2} m^{-2} \simeq 10^{12} M_\odot$ obtained for WDM particles with mass m in the keV scale. The fact that a WDM particle with mass in the keV scale seems to be consistent with the observed properties of dwarf and large galaxies provides a strong support to this dark matter candidate.

Keywords: self-gravitating systems; phase transitions; evaporation; keV warm dark matter

1. Introduction

The thermodynamics of astrophysical systems is hallmarked by the incidence of a long-range interaction like Newtonian gravitation. This interaction is directly responsible about the occurrence of anomalies like gravothermal collapse and negative heat capacities [1–8]. Other difficulty associated with this interaction is the incidence of evaporation, namely, the existence of a finite energy threshold where the constituents of an astrophysical system can escape out from its own gravitational field [9–24]. Under these conditions, astrophysical systems in Nature are not found in thermodynamic equilibrium. Nevertheless, these systems can reach a quasi-stationary evolution that is possible to describe by methods of statistical mechanics and thermodynamics.

An astrophysical model that combines both quantum and evaporation effects is the called *fermionic King model* [24]. The corresponding distribution function associated to this model was introduced empirically by Ruffini and Stella in the context of dark matter halos problems [20], and independently by Chavanis [21], who justified it from a kinetic theory based on the fermionic Landau equation. In recent years, Chavanis and co-workers [22–24] performed an extensive analysis of this model concerning the role of quantum degeneration. In a precedent paper [25], this same model was revisited by Velazquez and Espinosa-Solis in order to clarify the role of the total mass M on the thermodynamic stability. It

was shown that the competition among quantum and evaporative effects leads to the existence of certain critical bounds for the total mass M that control the character of gravothermal collapse. Besides the *upper bounds* of the total mass associated with quantum-relativistic considerations [26–30], this model predicts that the total mass of astrophysical systems could exhibit *lower bounds* due to the incidence of quantum and evaporation effects. After reviewing several aspects about the thermodynamics of self-gravitating systems that undergo the evaporation (escape) of their constituents, results obtained from the fermionic King model will be applied here to the study of warm dark matter in galactic halos. Inspired on precedent studies on this subject by de Vega and coworkers [31–33], I shall derive new bounds for the mass of WDM particles considering the observed properties of dwarf galaxies. Additionally, I shall discuss some connections concerning the formation of degenerate core via gravothermal collapse, the supper-massive black holes that are reported to exist at the center of galaxies and the existence of WDM particles with mass in the keV scale.

2. Antecedents

2.1. Thermodynamic Effects of Evaporation

The evaporation of constituents implies an out-of-equilibrium situation, so that, there is no unique way to account for this phenomenon throughout astrophysical models. Among all proposals considering evaporation effects, King model [11–14] has received a considerable attention in the literature since they provide a quite realistic description of the star distributions of globular clusters, as well as brightness surfaces of elliptical galaxies. Although King model is recovered as a limit case of fermionic King model reviewed in the Section 2.3 below, it is merely one of possible models that accounts for evaporation effects. It is worth to say that critical bounds for the total mass of degenerate self-gravitating systems are *model-dependent* since they depend on the specific way one deals with the constituents evaporation.

Recently, Gomez-Leyton and Velazquez have shown that King model belongs to the family of lowered isothermal models [15]

$$f(\mathbf{r}, \mathbf{p}|\beta, \varepsilon_c, \gamma) = AE(x, \gamma), \tag{1}$$

which they referred to as γ-exponential models. Here, $x \equiv \beta[\varepsilon_c - \varepsilon(\mathbf{r}, \mathbf{p})]$, β is the inverse temperature parameter, ε_c is the cutoff (escape) energy, while $\varepsilon(\mathbf{r}, \mathbf{p}) = \mathbf{p}^2/2m + m\phi(\mathbf{r})$ denotes the individual mechanical energy for a particle with mass m and momentum $\mathbf{p}$ that is located at the position $\mathbf{r}$, with $\phi(\mathbf{r})$ being the gravitational potential. This phenomenological proposal exploits and extends the truncation of power-expansion of exponential function discussed by Davoust [34] considering a continuous deformation parameter γ as follow:

$$E(x, \gamma) = \sum_{k=0}^{+\infty} \frac{1}{\Gamma(\gamma + 1 + k)} x^{\gamma+k}, \tag{2}$$

where $\Gamma(x)$ in the Gamma function. The mathematical behavior of this last function is shown in Figure 1. Equation (1) includes a set of models already employed in astrophysics, such as the models of Woolley [16] (for $\gamma = 0$), King (for $\gamma = 1$), Wilson [17] (for $\gamma = 2$), polytropes [35,36] (in the limit of high energies) and Plummer [37] (a marginal case of polytropes where $\gamma \to 7/2$). This family of models was generalized by Gieles and Zochi to include rotation anisotropy and the presence of a mass-spectrum [38].
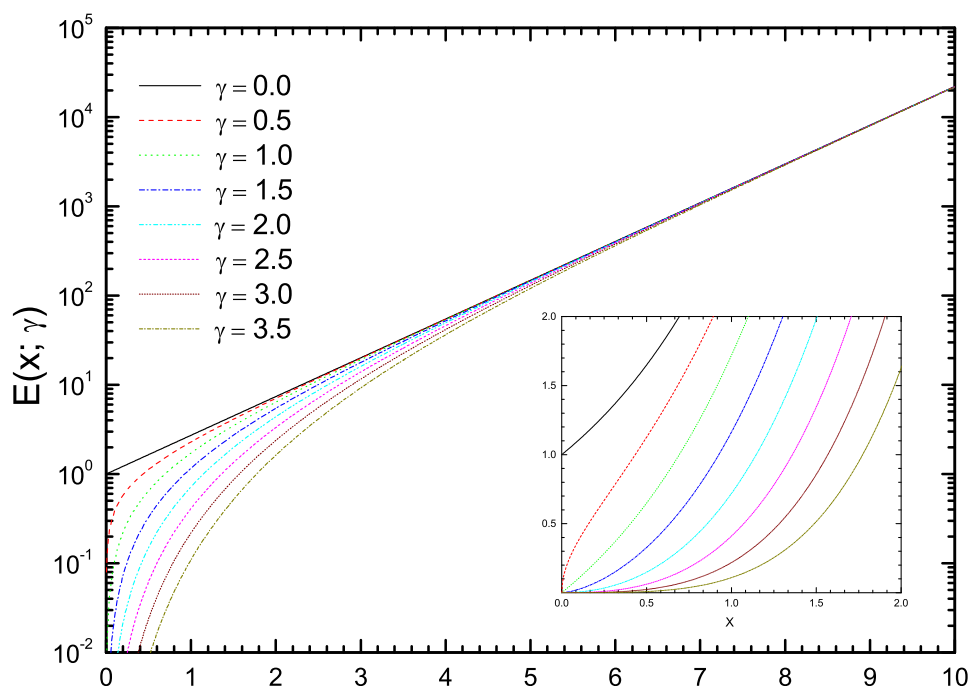
Figure 1. Behavior of $\gamma-$exponential function (2). Main panel: this function converges towards usual exponential function for large values of its argument x. Inset panel: it drops to zero when $x \to 0^+$ following a power-law of the type $E(x, \gamma) \propto x^\gamma$. The $\gamma-$exponential function is just the *fractional derivative* of the exponential function, $E(x, \gamma) \equiv d^\gamma(e^x)/dx^\gamma$. After [15].

The γ-exponential models enable a *panoramic view* about the incidence of evaporation on the thermodynamics of astrophysical systems [19]. The truncation in the one-body distribution function (1) is described by two parameters: (a) the energy threshold ε_c that defines the system size via the tidal radius R, and (b) the deformation parameter γ that drives the deviation of the one-body distribution (1) from the isothermal Maxwell-Boltzmann profile:

$$f_{MB}(\mathbf{r}, \mathbf{p}|\beta) \sim \exp[-\beta\varepsilon(\mathbf{r}, \mathbf{p})] \tag{3}$$

throughout the power-law truncation of with exponent γ at the cutoff energy ε_c. Due to the divergence of polytropes when the exponent $n > 5$ [36], the admissible values of the deformation parameter γ belong to the interval $0 \le \gamma \le 7/2$. The thermodynamics of these models is qualitatively similar to the one shown by King model for the cases where $0 < \gamma \le \gamma_c \simeq 2.1$. However, nontrivial consequences are found for the cases where $\gamma_c \le \gamma < 7/2$, such as the divergence of the energy of gravothermal collapse and the existence of multiples branches of stabilities. As already shown by Gomez-Leyton and Velazquez [19], the thermodynamic effects of evaporation strongly depend on other dynamical factors, such as the existence of mass-spectrum for the constituents.

In the same fashion that King model is one of possible γ-exponential models that account for the incidence of evaporation for classical self-gravitating systems, the fermionic King model is just one of possible models that describe evaporation effects for systems of self-gravitating fermions. This particular model will be employed later in Section 3.2 to obtain new bounds for the mass m of warm dark matter particles (WDM). In general, such bounds will depend on the concrete truncation of one-body distribution function at the escape energy ε_c, which means that this problem far to be fully solved in the present study. I shall return to this question at the end of conclusion section.

2.2. Concerning the Thermodynamic Limit

The thermodynamics of astrophysical systems exhibits a great sensibility to the external conditions. A good illustration about this very fact was discussed years ago by de Vega and Sanchez [5], who showed that the thermodynamics depends on the *shape of the container* that is employed to confine a self-gravitating system (an unrealistic theoretical assumption to avoid the escape of constituents). This behavior is radically different from the ones observed for the case of extensive systems (large systems with short-range interactions). Conventionally, the incidence of *surface effects* can be neglected in comparison with bulk effects whenever the system size (e.g., the number of particles N or the volume V) is very large. For example, the boiling temperature of water can depend on the environmental pressure p, but it does not depend on the volume of container or its shape whenever one considers the thermodynamic limit:

$$N \to +\infty: U/N = const \text{ and } V/N = const. \tag{4}$$

Due to the long-range character of gravitation, however, one cannot affect a part of the astrophysical systems without disturbing the whole system. By themselves, this feature is the reason why the thermodynamic of astrophysical systems is so rich and challenging. Each realistic assumption introduced into a theoretical analysis can produce significant changes in the thermodynamics of the proposed model. Essentially, every external or internal condition matters in this scenario: the initial conditions of microscopic dynamics, the incidence of quantum and relativistic effects, the presence of a mass spectrum or the evaporation (escape) of constituting particles, the asymmetry of distributions due to the system proper rotation, etc.

The thermodynamic limit (4) is not relevant in astrophysics due to the long-range character of gravitation. For the particular case of the self-gravitating gas of non-relativistic point particles, the question of the thermodynamic limit has not reached a consensus in the literature (different proposals have been made for this class of systems). This problem was recently revisited in Ref. [39], where I provided a series of arguments in favor of the thermodynamic limit:

$$N \to \infty: \frac{U}{N^{7/3}} = const, VN = const. \tag{5}$$

This same thermodynamic limit also applies for the case of fermionic King model [25]. In fact, the relevance of this thermodynamic limit for these type of systems was early demonstrated by Hertel and Thirring [40] and recovered from simpler (scaling) arguments in Section 7.1. of [8] and in Appendix B of [41] where it was called the *quantum thermodynamic limit*. For the sake of the self-consistency of the paper, let us recall some arguments leading to this thermodynamic limit as well as its applicability conditions.

Plummer model is presumably the simplest and oldest toy model that includes a truncation of the energy spectrum due to the incidence of evaporation [37]. The later one can be considered as a marginal particular case with $n = 5$ of polytropic models [35]:

$$f_n(\mathbf{r}, \mathbf{p}) = \begin{cases} A_n \mathcal{E}^{n-3/2}, & \text{if } \mathcal{E} > 0, \\ 0, & \text{if } \mathcal{E} \leq 0, \end{cases} \tag{6}$$

where $\mathcal{E} = \varepsilon_c - \varepsilon(\mathbf{r}, \mathbf{p})$. Its density profile is infinitely extended in the space:

$$\rho_P(r) = \frac{3M}{4\pi a^3} \left(1 + \frac{r^2}{a^2}\right)^{-5/2}, \tag{7}$$

but it exhibits finite total mass M and characteristic radius a. Its associated potential is also analytical:

$$\phi_P(r) = -\frac{GM}{\sqrt{a^2 + r^2}}. \tag{8}$$

Accordingly, its energy threshold for the escape of particles $\varepsilon_c \equiv 0$, which means that Plummer model describes *an isolated* self-gravitating gas of non-relativistic point particles. Considering the normalization condition (N is number of particles):

$$N = \int f_P(\mathbf{r}, \mathbf{p}) \frac{d^3\mathbf{r}\,d^3\mathbf{p}}{(2\pi\hbar)^3} \tag{9}$$

and calculating the total energy U:

$$U = \int \left(\frac{1}{2m}\mathbf{p}^2 + \frac{1}{2}m\phi(\mathbf{r}), \right) f_P(\mathbf{r}, \mathbf{p}) \frac{d^3\mathbf{r}\,d^3\mathbf{p}}{(2\pi\hbar)^3}, \tag{10}$$

one obtains that the characteristic radius a is related to the total energy U as:

$$a = \frac{3\pi}{64} \frac{GM^2}{(-U)}. \tag{11}$$

This last result implies that Plummer model does not exhibit any characteristic energy or length (it is scale independent).

The relevance of the thermodynamic limit (5) for the system of self-gravitating non-relativistic point particles can be particularly shown by considering the entropy associated with Plummer model:

$$S = -k \int f_P(\mathbf{r}, \mathbf{p}) \log f_P(\mathbf{r}, \mathbf{p}) \frac{d^3\mathbf{r}\,d^3\mathbf{p}}{(2\pi\hbar)^3}. \tag{12}$$

Avoiding exact mathematical calculations, one can obtain the following estimation [39]:

$$S \sim \frac{3}{2} Nk \log\left[\frac{G^2 m^5}{2\hbar^2} \frac{N^{7/3}}{(-U)} \right]. \tag{13}$$

The mathematical form of this entropy is consistent with the following thermodynamic limit:

$$N \to \infty: \quad \frac{S}{N} = const, \quad \frac{U}{N^{7/3}} = const, \tag{14}$$

which ensures the extensivity of the entropy. The same scaling properties are also applicable the case of non-relativistic self-gravitating fermions [40], which evidences that this thermodynamic limit does not depend on classical or quantum description for the case of self-gravitating non-relativistic point particles.

Let us now exploit the Plummer model to discuss the restricted applicability of the thermodynamic limit (5). The calculation of the entropy using formula (12) accounts for the quantum-classical approximation (the presence of the factor $(2\pi\hbar)^3$ dividing the configuration space volume $d^3\mathbf{r}\,d^3\mathbf{p}$). From the estimation (13), one verifies the existence of the following characteristic energy:

$$|U_c| \sim \frac{G^2 m^5}{\hbar^2} N^{7/3}. \tag{15}$$

The later one appears when quantum correlations turn important in the innermost regions described by Plummer profile (7). Considering the characteristic momentum:

$$p \sim \sqrt{2m(-U)/N} \tag{16}$$

and the radius a given by (11), de Broglie length λ turns comparable to the inter-particle distance:

$$\lambda = \frac{\hbar}{p} \sim \left(\frac{a^3}{N}\right)^{1/3} \tag{17}$$

for energies of order of the characteristic energy (15). For this energy scale, the classical non-relativistic Plummer model losses its applicability, and the same one should be extended by a sort of *fermionic Plummer model* (A generalized family of models for self-gravitating systems of non-relativistic fermions that undergo evaporation is suggested at the end of the paper: the fermionic γ-exponential models. The fermionic Plummer model should be the marginal case of $\gamma = 7/2$ of this family of generalized models). While the quantum description does not restrict the application of the thermodynamic limit (5), this result loses its validity in the relativistic limit. In particular, the characteristic energy (15) should not overcome the rest energy of the system

$$|U_c| \sim \frac{G^2 m^5}{\hbar^2} N^{7/3} < Nmc^2. \tag{18}$$

Accordingly, the results of non-relativistic approximation lost their applicability when total mass $M = Nm$ of the self-gravitating system approaches the characteristic mass M_c

$$M_c \sim \left(\frac{\hbar c}{G}\right)^{3/2} \frac{1}{m^2}. \tag{19}$$

By itself, the previous argument implies that the thermodynamic limit (14) is only relevant within a non-relativistic approximation. Replacing the generic mass m by the mass of hydrogen atoms H, one immediately obtains the characteristic mass constant:

$$M_c = \left(\frac{\hbar c}{G}\right)^{3/2} \frac{1}{H^2} \sim 29.2 M_\odot \tag{20}$$

that appears in stability limits of stars [27–30].

2.3. Thermodynamics of Fermionic King Model at Constant Total Mass

The one-body distribution proposed by Ruffini and Stella [20] can be expressed into the following form:

$$f(\mathbf{r}, \mathbf{p}|\beta, \varepsilon_c) = \frac{e^{\beta[\varepsilon_c - \varepsilon(\mathbf{r}, \mathbf{p})]} - 1}{\alpha + e^{\beta[\varepsilon_c - \varepsilon(\mathbf{r}, \mathbf{p})]}} H[\varepsilon_c - \varepsilon(\mathbf{r}, \mathbf{p})]. \tag{21}$$

Here, $H(x)$ is Heaviside step function, $\beta = 1/kT$ represents the inverse temperature parameter, $\varepsilon_c = m\phi_s$ denotes the energy threshold for the escape of particles, and $\phi_s = -GM/R$ is the surface potential. Finally, α is a dimensionless positive parameter associated with normalization of the one-body distribution, which ensures the inequality $f_{FDT}(\mathbf{r}, \mathbf{p}|\beta) \leq 1$. The ansatz (42) provides a suitable interpolation between the known Fermi-Dirac distribution:

$$f_{FD}(\mathbf{r}, \mathbf{p}|\beta) = \frac{1}{e^{\beta[\varepsilon(\mathbf{r}, \mathbf{p}) - \varepsilon_F]} + 1} \tag{22}$$

in the limit of low energies and the quasi-stationary one-body distribution associated with King models [11–14]:

$$f_K(\mathbf{r}, \mathbf{p}|\beta, \varepsilon_c) = \frac{1}{\alpha} \left[e^{\beta[\varepsilon_c - \varepsilon(\mathbf{r}, \mathbf{p})]} - 1\right] H[\varepsilon_c - \varepsilon(\mathbf{r}, \mathbf{p})] \tag{23}$$

in the classical non-degenerate limit. Notice that ε_F denotes the Fermi energy, which enable us to rewrite the normalization constant α as $\alpha \equiv e^{\beta(\varepsilon_c - \varepsilon_F)}$. Accordingly, the limit

of low energies (22) corresponds to the condition $\beta[\varepsilon_c - \varepsilon(\mathbf{r}, \mathbf{p})] \gg 1$, while the classical non-degenerate limit (23) is given by the conditions $\alpha \gg 1$ and $f_{FDT}(\mathbf{r}, \mathbf{p}|\beta, \varepsilon_c) \ll 1$. The normalization parameter α characterizes the degree of degeneration of the astrophysical situation described by this model.

As already shown in the precedent work [25], the thermodynamics of fermionic King model is driven by the incidence of two characteristic lengths: the tidal radius R and the Fermi radius R_F

$$R_F^3 = \frac{1}{M} \frac{9\pi^4}{2g^2} \frac{\hbar^6}{G^3 m^8} c^2. \tag{24}$$

Here, $g = 2s + 1$ is the spin multiplicity, the total mass M, and the numerical constant $c = 0.9156$. The tidal radius R defined the confinement region $r < R$ where the system is trapped by its gravitational field. This characteristic length dominates the high energy branch that ranges from the point of gravothermal collapse u_c up to point of evaporation disruption u_c (the same branch observed in classical King model). The Fermi radius R_F determines the low energy branch that corresponds to post-collapse states with degenerate fermion cores. These two characteristic lengths can be employed to introduce the mass ratio parameter θ and the Fermi mass M_F as follows:

$$\theta = \left(\frac{R_F}{R} \right)^3 \equiv \frac{M_F}{M} \text{ and } M_F \equiv \frac{1}{R^3} \frac{9\pi^4}{2g^2} \frac{\hbar^6}{G^3 m^8} c^2. \tag{25}$$

The mass ratio parameter characterizes the system degeneracy due to the competition among quantum and evaporation effects, while the Fermi mass M_F is the total mass corresponding to a self-gravitating degenerate system whose Fermi radius R_F is equal to the tidal radius R. One could expect that the Fermi radius R_F for a self-gravitating degenerate system of fermions should not overcome the value of the tidal radius R. In any case, the possible existence of an upper limit θ_m for the mass ratio parameter θ anticipates that the fermionic King model should exhibit *a lower bound mass for the system stability against evaporation disruption*.

Introducing the dimensionless potential $\Phi(\mathbf{r})$ and the dimensionless radius $\xi = \xi_c r / R$:

$$\Phi(\mathbf{r}) = \beta m[\phi_s - \phi(\mathbf{r})], \tag{26}$$

one obtains the following differential equation:

$$\frac{1}{\xi^2} \frac{d}{d\xi} \left[\xi^2 \frac{d\Phi(\xi)}{d\xi} \right] = -4\pi F \left[\Phi(\xi), \mu, \frac{3}{2} \right], \tag{27}$$

which enable us to derive the spherical solutions of fermionic King model. The function $F(\Phi, \mu, \nu)$:

$$F(\Phi, \mu, \nu) \equiv \frac{1}{\Gamma(\nu)} \int_0^\Phi \frac{e^{\Phi - x} - 1}{1 + e^{\Phi - x - \mu}} x^{\nu - 1} dx \tag{28}$$

is the *Fermi-King integral*, which depends on the *degeneration parameter* $\mu = \ln \alpha$. The integration of this problem requires both the boundary conditions and the regularity conditions at the origin:

$$\Phi(0) = \Phi_0, \frac{d\Phi(0)}{d\xi} = 0, \Phi(\xi_c) = 0 \text{ and } \xi_c \frac{d\Phi(\xi_c)}{d\xi} = -\eta = -\beta \frac{GMm}{R}, \tag{29}$$

where η is the dimensionless inverse temperature. Details of numerical calculations and expressions of thermodynamic observables and potentials will be omitted here in the sake of brevity. It is important to mention that Chavanis and co-workers addressed in Ref. [24] the thermodynamics of this model *at constant degeneration parameter μ*. In my precedent paper with Espinoza-Solis [25], we have discussed the thermodynamics of this model *at constant total mass M* (or constant mass ratio parameter θ), whose results significantly differ

from the precedent study. For the convenience of the readers, some additional notes are presented in the Appendix A to clarify the existing differences.

The numerical computation of the dependence $\mu = \mu(\Phi_0, \theta)$ and the associated caloric curves η *versus* u^* at constant total mass M are shown in Figure 2, where $u^* = -GM^2/RU$ is the dimensionless inverse energy, with U being the total energy. It was included here the caloric curve corresponding to the classical King model for comparative purposes. The observed thermodynamic dependencies can be grouped into three regions of values for the mass ratio parameter θ, which are distinguished among them by a different qualitative behavior of the caloric curves:

- **The region I**: the interval $0 \leq \theta < \theta_1 \simeq 1.12 \times 10^{-7}$ (black curves). The gravitational collapse of fermionic King model represents a discontinuous microcanonical phase transition, and its thermodynamics exhibits a branch with negative heat capacities. The classical King model that appears when $\mu \to +\infty$ corresponds to the infinite mass limit $\theta \to 0$. In terms of the total mass M, this region corresponds to situations with high total masses, the interval $M_1 < M < +\infty$, where $M_1 = M_F/\theta_1 \simeq 8.9 \times 10^6 M_F$.

- **The region II**: the interval $\theta_1 \leq \theta < \theta_2 \simeq 1.10 \times 10^{-2}$ (red curves). The gravitational collapse of fermionic King model turns a continuous microcanonical phase transition, and its thermodynamics exhibits a branch with negative heat capacities. In terms of the total mass M, this region corresponds to situations with intermediate total masses, the interval $M_2 < M \leq M_1$, where $M_2 = M_F/\theta_2 \simeq 90.9 M_F$.

- **The region III**: the interval $\theta_2 \leq \theta < \theta_m \simeq 4.0$ (green curves). The gravitational collapse of fermionic King model is a continuous microcanonical phase transition, and its thermodynamics does not exhibit negative heat capacities. In terms of the total mass M, this region corresponds to situations with low total mass, the interval $M_3 < M \leq M_2$, where $M_3 = M_F/\theta_m \simeq ¼ M_F$.
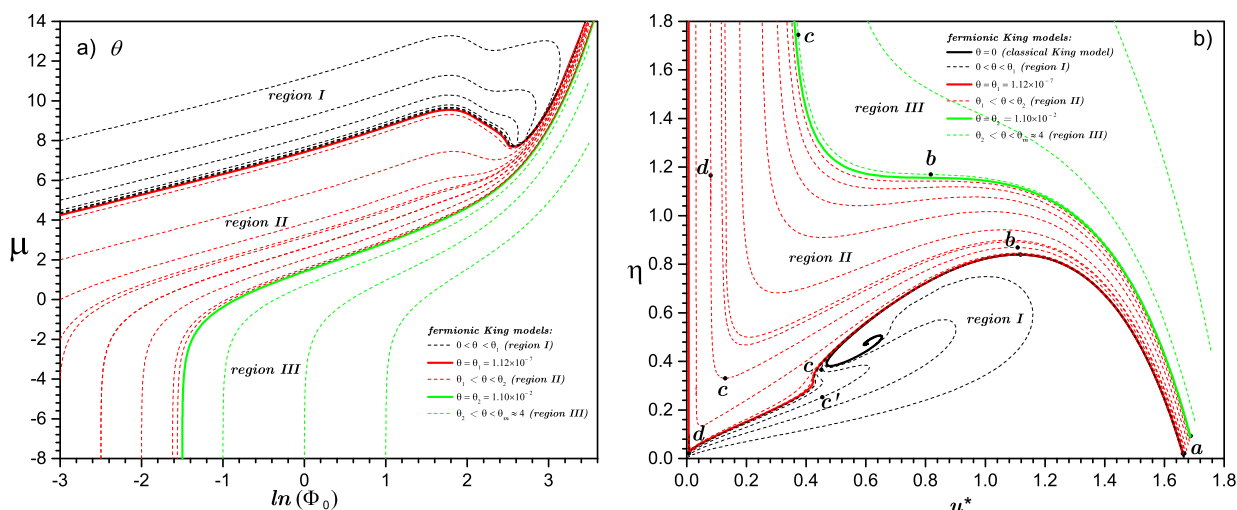

Figure 2. (**a**): Contour maps of the mass ratio parameter $\theta = M_F/M$ [see in Equation (25)] in the plane of integration parameters $[\Phi_0, \mu]$ of the Poisson problem (27), which were obtained from numerical procedures designed to fulfil this purpose. Here, $\mu = \ln \alpha$ is the degeneration parameter defined from the normalization constant α in Equation (42); Φ_0 is the central value of the dimensionless potential (26). Notice that for each value of the degeneration parameter μ there exist *infinite values for the mass ratio parameter* θ since this quantity also depends on the dimensionless potential Φ_0, $\theta = \theta(\Phi_0, \mu)$. This very fact implies that thermodynamics of fermionic King model *at constant degeneration parameter* μ differs from its thermodynamics *at constant mass ratio* θ (or constant total mass M). (**b**): Corresponding caloric curves at constant mass ratio parameter θ in terms of the dimensionless inverse temperature $\eta = \beta GMm/R$ and the auxiliary variable $u^* = -GM^2/RU$ defined from the total energy U. One can observed the existence of three regions with different thermodynamic behavior. The points (a, b, c, c', d) are some notable configurations. Among them, it is remarkable the case of configurations (c, c') over the curve with $\theta = 2.84 \times 10^{-8}$ (region I), which exhibit the same energy *but different temperatures*. The during discontinuous jump from the profile c towards the profile c', the system temperature grows and there exist a redistribution of the mass that leads to the formation of a dense degenerate core. After [25].

The model does not exhibit solutions for values of the mass ratio parameter $\theta > \theta_m$. As already commented, the value θ_m implies the minimum mass $M_3 = M_F/\theta_m$ for the system stability. Accordingly, if M is lower than the one quarter of the Fermi mass, the effective repulsive forces associated to Fermi exclusion principle will overcome the system gravitation, and the same one will undergo a very intense evaporation until dissipating as a whole.

The phenomenology of the caloric curves at constant total mass M discussed here is rather similar to the one the thermodynamics of this model at constant degeneration parameter μ [24,25]. In fact, the identification of three regions in the phase diagram of the self-gravitating Fermi gas has been also reported in other studies [8,22], which are related to the existence of canonical and microcanonical critical points in the self-gravitating Fermi gas model. The originality of present approach concerns to highlight the importance of the total mass in the thermodynamic stability of this model. There are other aspects that are discussed in more details in the precedent work [25], like the formation of degenerate core via gravothermal collapse. Chavanis and coworkers argued in section VI of Ref. [24] that the formation of degenerate core falls into unstable branch of caloric curves and this type of structures (fermion balls) should not be observed at the center of dark matter haloes (solutions that they referred as *embryonic phase*). However, the previous claim is not fully rigorous since solutions with degenerate cores are also present in stable blanches. According the caloric curves shown in the right panel of Figure 2, the configurations (c, c') fall on stable branches of the caloric curve with $\theta = 2.84 \times 10^{-8}$ (region I). A discontinuous jump from the profile c towards the profile c' involves a *violent redistribution* of the mass that leads to the formation of a dense degenerate core with a warmer polytropic halo. In fact, other type of structures can be observed in the thermodynamics of this model, like stable solutions with degenerate core, *isothermal gas envelop* and a polytropic halo [25].

3. Application to Dark Matter Halos

3.1. Incidence of Evaporation Effects

Recently, the macroscopic effects of quantum degenerated astrophysical systems have been applied by de Vega and co-workers to the study of dark matter (DM) halos in galaxies [31–33]. According to these studies, the quantum effects in warm dark matter (WDM) could turn important near the galactic centers, overall for the case of dwarf galaxies (whose content of DM is much more significant). By itself, this claim explains why classical N-body simulations fail to describe galactic cores and their sizes; e.g., the appearance in simulations of cuspid distributions like NFW-profile [42]:

$$\rho_{NFW}(r) = \frac{\rho_0 r_s^3}{r(r_s + r)^2},$$
(30)

where ρ_0 and r_s are fitting parameters, which is divergent at the origin as the isothermal sphere:

$$\rho(r) = \frac{\sigma_v^2}{2\pi G r^2},$$
(31)

where σ_v^2 is the velocity dispersion. Profiles with this type of divergences reflect the gravitational collapse of self-gravitating system of classical non-relativistic point particles. However, such divergences are absent in self-gravitating systems of fermions [24,25], which predict the formation of a *core-halo structure* with a degenerate core for low energies. In other words, WDM may be capable to solve the called *cusp-core problem* [43].

In the study of dark matter in galaxies, de Vega and co-workers considered a Fermi-Dirac distribution (22), but they do not account for the incidence of evaporation. Since a Fermi-Dirac distribution converges towards the classical Maxwell-Boltzmann distribution (3) for large energies, their theoretical profiles recover the isothermal sphere tail $1/r^2$ for large distances (corresponding to a linear-divergent total mass). To avoid the long-range divergence of gravitation, they restricted calculations to a finite region of the space below the radius

r_{200} (the radius where the mass density equals 200 times the mean DM density), which is a typical length employed in studies of dark matter halos [44]. Considering precedent studies concerning the comparison of empirical rotation curves of large galaxies using the Burkert profile (r_h denotes the halo radius and ρ_0 the central density):

$$\rho_B(r) = \frac{\rho_0 r_h^3}{(r_h + r)(r_h^2 + r^2)}, \tag{32}$$

de Vega and co-workers have obtained a good agreement among their theoretical profiles in the classical regime within halos cores for distances $r < 2r_h$ [33]. As expected, discrepancies turn significant for larger distances since Burkert profile (32) predicts tails $1/r^3$ (corresponding to a logarithmic-divergent total mass).

Generally speaking, empirical profiles with tails $1/r^\alpha$ with exponent $\alpha = 3 - 5$ can be explained by classical astrophysical models considering an evaporation truncation [23]. The fact that observed DM halos can be described using empirical profiles with these tails is an indicator about the incidence of evaporation effects. In a similar way as a globular cluster exhibits a tidal radius due to the gravitational influence of its host galaxy, the galaxies them-selves should exhibit tidal radius due to the gravitational influence of other galaxies in galactic clusters. For illustrative purposes, it is shown in Figure 3 a comparison between a density profile near gravothermal collapse corresponding to King model ($\gamma = 1$) and the Burkert profile (32) with fitting radius $r_h = 0.01R$. Despite the existing of small discrepancies in the innermost regions, the fit is reasonably good for distances $r < 25r_h = 0.25R$. It is worth to mention that this particular King profile exhibits an *isothermal core*. Additionally, it is also shown in this figure a second King profile for configurations with higher energy (near the point of isothermal collapse), which does not exhibit an isothermal core [15]. For this case, the fit is much better using an empirical Plummer-like profile:

$$\rho_{Pl}(r) = \frac{\rho_0 r_h^{2n}}{(r_h^2 + r^2)^n}, \tag{33}$$

with $n = 2.1$ and $r_h = 0.16R$, which is reasonably good for distances $r < 2.5r_h = 0.40R$. As expected, the high energy King profiles undergo a major incidence of evaporation, which correspond to empirical profiles (33) with larger exponent n. According to these examples, Burkert profile (32) not only allows us to infer the existence of evaporation effects, but also that it corresponds to configurations with isothermal cores, which are observed for low energies close to gravitational collapse only. This fact was previously noticed by Chavanis and co-workers in Ref. [23], who presented a more complete comparison among distributions derived from the classical King model and empirical profiles with tails $1/r^\alpha$. Fermionic King model should also provide a good fit of dark matter distributions of galaxies since it contains the classical King model as a limit case. Of course, the available observational data DM halos might not be confident to show the existence (or nonexistence) of a finite tidal radius R in the outermost regions.
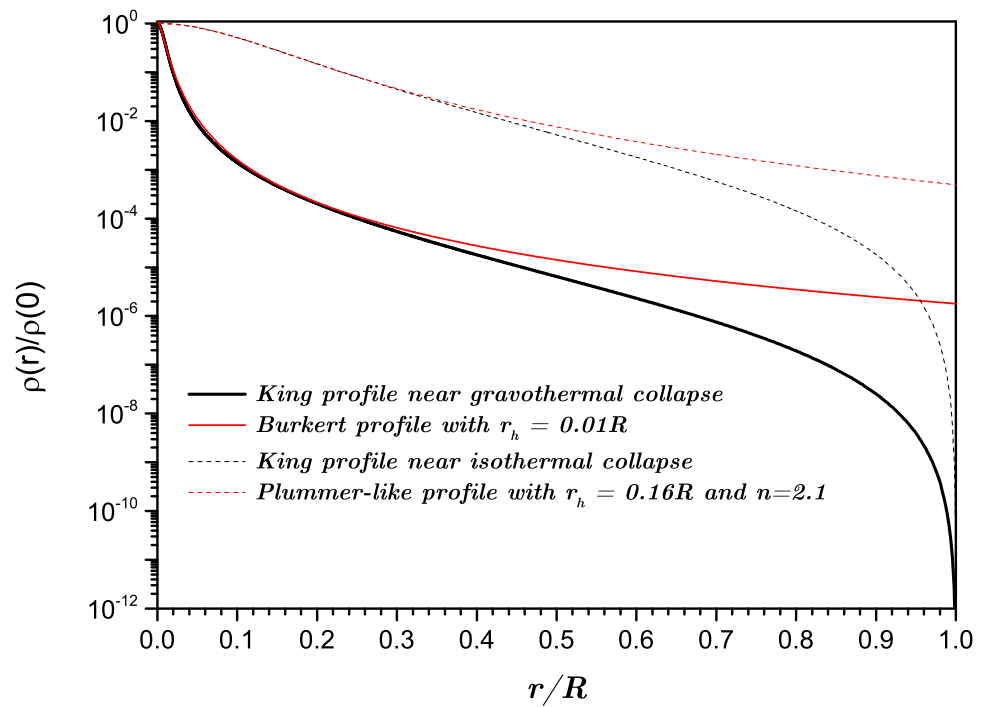
Figure 3. Comparison of two King profiles with and without isothermal cores, and the empirical profiles of Burkert (32) and Plummer-like (33). Here, *R* denotes the tidal radius.

3.2. New Bounds of WDM Particles Mass m from Fermionic King Model

To reproduce the smaller observed structures, different studies using *N*-body simulations suggested that the WDM particle mass should be in the keV scale [45–51]. Among different candidates for WDM particles are the called *sterile neutrinos* with masses of order of $m \sim$ keV [52]. Considering the reported data of dwarf galaxy Willman 1, de Vega and co-workers estimated that the WDM particle mass *m* is approximately around 2 keV [31]. Their analysis was focussed on the upper bound of the phase space density:

$$Q(\mathbf{r}) = \frac{\rho(\mathbf{r})}{\sigma^3(\mathbf{r})} \qquad (34)$$

that arises in the degenerate limit, where $\rho(\mathbf{r})$ is the density and $\sigma(\mathbf{r})$ the velocity dispersion.

As already commented, the mass bound derived by de Vega and co-workers disregards the incidence of evaporation. Instead, they invoked a conventional recipe that is rather equivalent to the use of box to enclose the self-gravitating system [2]. Although this argument is theoretically useful to perform estimations, it is clearly *nonphysical* for self-gravitating systems like galaxies, where the escape of constituents is unavoidable process. The fermionic King model provides a more realistic approach to these situations. The competition of evaporation and quantum effects imply the following upper bound for the mass-ratio parameter:

$$\theta = \frac{M_F}{M} \leq \theta_m \simeq 4, \qquad (35)$$

which depends on the total mass *M* and the tidal radius *R* of the system. For systems with masses below the lower bound $M_3 = \frac{1}{4} M_F$, the gravitation cannot retain their constituents and they suffer a complete and violent evaporation disruption. This collective instability appears when fermionic quantum pressure overcomes gravitation within the region enclosed by the tidal radius *R*. If DM halos are composed of fermionic WDM particles, the mass-ratio of compact dwarfs galaxies could be close to this upper bound, so that, they should exhibit strong predominance of quantum degeneration [31–33].

Let us assume the value $g = 2$ and the rough estimation $R \simeq 100 r_h$ for the tidal radius R from the halos radius of Burkert profile r_h derived from the fit of Figure 3. The mass-ratio (25) can be expressed as follows:

$$\theta = \theta_h \left(\frac{2\text{keV}}{m} \right)^8 ,\tag{36}$$

where the pre-factor θ_h is given by:

$$\theta_h \simeq 17 \left(\frac{10^6 M_\odot}{M} \right) \left(\frac{pc}{r_h} \right)^3 .\tag{37}$$

Notice that the pre-factor θ_h is just the mass-ratio corresponding to a WDM particle with $m = 2$ keV. The calculations shown in the Table 1 are based on the same observational data considered by de Vega and co-workers in Ref. [31]. According to these calculations, Willman 1 is the dwarf galaxy that exhibits the largest value of the mass ratio parameter θ, and hence, the one whose internal conditions are closest to the evaporation disruption associated to the upper bound (35):

$$\theta = 0.085 \left(\frac{2\text{keV}}{m} \right)^8 \leq 4.\tag{38}$$

The previous inequality implies WDM particles with masses $m \geq m_{\min} = 1.2$ keV. Considering this lower bound, the corresponding maximum values θ_{max} of the mass ratios for most of galaxies shown in Table 1 correspond to the region I, where $0 < \theta < \theta_1 = 1.12 \times 10^{-7}$. For these cases, the thermodynamics of fermionic King model predicts a gravothermal collapse for low energies with the character of a discontinuous microcanonical phase transition. Those galaxies whose mass ratios θ belong to the interval $\theta_1 < \theta < \theta_2 \simeq 1.10 \times 10^{-2}$ correspond to the region II, where gravothermal collapse for low energies is a continuous microcanonical phase transition. Systems under these conditions are more gravitationally stable. In fact, their thermodynamics is dominated by gravitation because of they exhibit states with negative heat capacities.

Curiously, Willman 1 is the only dwarf galaxy of Table 1 that could belong to the region III, where the mass-ratio values are located inside the interval $\theta_2 < \theta \leq \theta_m \simeq 4.0$. This possibility requires WDM particle with mass m within the range:

$$m_{\min} = 1.2 \text{ keV} \leq m \leq m_{\max} = 2.6 \text{ keV}.\tag{39}$$

If this is correct, then the internal conditions of Willman 1 are exceptionally different from the rest of the galaxies. The progressive lost of mass and energy associated with the escape of its constituents (by the incidence of tidal forces) can eventually drive Willman 1 towards its complete evaporation disruption. The so rare character of dwarf galaxies belonging to the region III suggests that a stellar system under these conditions should undergo a fast evolution via the evaporation of its constituents. Studies concerning the dynamics under evaporation for systems of self-gravitating fermions are required to estimate the associated evolution times. At this point, it is also reasonable that Willman 1 actually falls into the region II (more stable system), which requires that the mass of WDM particles obeys the bound $m > 2.6$ keV.

Table 1. Observed values of the DM halos parameters [r_h (radius), ρ_0 (central density) and M_h (mass)] employed by Destric and co-workers covering from ultracompact galaxies to large spiral galaxies (obtained from [53–62]). Assuming that the dwarf galaxy Willman 1 belongs to the region III of fermionic King model, $\theta_2 \le \theta \le \theta_m$, the mass m of WDM particles should belong to the range $m_{min} = 1.2\,\text{keV} \le m \le m_{max} = 2.6\,\text{keV}$. For this range of values, it was calculated the mass ratio $\theta = M_F/M$ for the rest of galaxies. Here, θ_f is the pre-factor of Equation (36), which corresponds to the mass ratio for a WDM particle with mass $m = 2\,\text{keV}$, while θ_{max} and θ_{min} are the mass ratios corresponding to the minimum and maximum masses m_{min} and m_{max}, respectively. The black values of the mass ratio θ belong to region I ($0 < \theta < \theta_1$), the red values belong to the region II ($\theta_1 < \theta < \theta_2$), while the green values to the region I ($\theta_2 < \theta \le \theta_m$).

Galaxy	$r_h\,[pc]$	$\rho_0\,\left[M_\odot pc^{-3}\right]$	$M_h\,\left[10^6 M_\odot\right]$	$\theta_{min}\,[m_{max}]$	θ_h	$\theta_{max}\,[m_{min}]$
Willman 1	19	6.3	0.029	1.1×10^{-2}	0.085	4.0
Segue 1	48	2.5	1.93	1.0×10^{-5}	8.0×10^{-5}	3.7×10^{-3}
Coma-Berenices	123	2.09	0.14	8.4×10^{-6}	6.5×10^{-5}	3.0×10^{-3}
Leo T	170	0.79	12.9	3.5×10^{-8}	2.7×10^{-7}	1.2×10^{-5}
Canis Venatici II	245	0.49	4.8	3.1×10^{-8}	2.4×10^{-7}	1.1×10^{-5}
Draco	305	0.5	26.5	2.9×10^{-9}	2.3×10^{-8}	1.0×10^{-6}
Leo II	320	0.34	36.6	1.8×10^{-9}	1.4×10^{-8}	6.6×10^{-7}
Hercules	387	0.1	25.1	1.5×10^{-9}	1.2×10^{-8}	5.5×10^{-7}
Boötes I	362	0.38	43.2	1.1×10^{-9}	8.3×10^{-9}	3.9×10^{-7}
Carina	428	0.15	32.2	8.7×10^{-10}	6.7×10^{-9}	3.2×10^{-7}
Ursa Major I	504	0.25	33.2	5.1×10^{-10}	4.0×10^{-9}	1.9×10^{-7}
Sculptor	480	0.25	78.8	2.5×10^{-10}	2.0×10^{-9}	9.1×10^{-8}
Leo IV	400	0.19	200	1.7×10^{-10}	1.3×10^{-9}	6.2×10^{-8}
Leo I	518	0.22	96	1.6×10^{-10}	1.3×10^{-9}	6.0×10^{-8}
Ursa Minor	750	0.16	193	2.7×10^{-11}	2.1×10^{-10}	9.8×10^{-9}
NGC 185	450	4.09	975	2.5×10^{-11}	1.9×10^{-10}	9.0×10^{-9}
Sextans	1290	0.02	116	8.8×10^{-12}	6.8×10^{-11}	3.2×10^{-9}
Canis Venatici I	1220	0.08	344	3.5×10^{-12}	2.7×10^{-11}	1.3×10^{-9}
Fornax	1730	0.053	1750	2.4×10^{-13}	1.9×10^{-12}	8.8×10^{-11}
NGC 855	1063	2.64	8340	2.2×10^{-13}	1.7×10^{-12}	7.9×10^{-11}
NGC 4478	1890	3.7	6.55×10^4	4.9×10^{-15}	3.8×10^{-14}	1.8×10^{-12}
Small Spiral	5100	0.029	6900	2.4×10^{-15}	1.8×10^{-14}	8.7×10^{-13}
NGC 3853	5220	0.77	2.87×10^5	5.4×10^{-17}	4.2×10^{-16}	1.9×10^{-14}
NGC 731	6160	0.47	2.87×10^5	3.3×10^{-17}	2.5×10^{-16}	1.2×10^{-14}
NGC 499	7700	0.91	1.09×10^6	4.4×10^{-18}	3.4×10^{-17}	1.6×10^{-15}
Medium Spiral	1.9×10^4	0.0076	1.01×10^5	3.2×10^{-18}	2.4×10^{-17}	1.1×10^{-15}
Large Spiral	5.9×10^4	2.3×10^{-3}	1.0×10^6	1.1×10^{-20}	8.3×10^{-20}	3.9×10^{-18}

3.3. The keV Scale and the Masses of Large Galaxies

According to the estimates shown in Table 1, most of galaxies exhibit mass-ratios θ compatible with the existence of a discontinuous gravothermal collapse for low energies. Such a gravitational instability leads to a violent redistribution of the mass that ends with the formation of a *degenerate core* of very small size. Accordingly, large galaxies could exhibit degenerate fermions cores of WDM particles. This idea is not new. Several authors have claimed in the past that WDM particles could provide a self-consistent model of dark matter that describes both the center and the halo of the galaxies [63,64]. It has been suggested that degenerate superstars composed of weakly interacting fermions in the 10 keV range could be an alternative to the supermassive black holes that are reported to exist at the center of galaxies [65–69]. The suggestion that DM halos may experience a discontinuous gravothermal catastrophe was also made by Chavanis et al in Ref. [24]. The mass of the DM halo above which the gravothermal catastrophe occurs was estimated by these authors as $M_h \sim 1.60 \times 10^7 M_\odot$ for a fermion mass $m = 1.23\,\text{keV}$. Their estimation, however, is not based on the fermionic King model itself, but a model of self-gravitating fermions enclosed into a box [8]. Despite this last model disregards the effects of evaporation, one observes

a reasonable agreement of this estimation with the results shown in Table 1. Apparently, the fermionic King model suggests the lower mass M_h should be slightly larger (for dwarf galaxies like Sculptor for a fermion with minimal mass $m = 1.2$ keV).

So far, it was only considered the behavior of WDM particles on the thermodynamics of these stellar systems. However, the presence of baryonic components (e.g., stars and inter-stellar gas) also plays an important role in this context. In the study with Gomez-Leyton concerning the γ-exponential models for a bi-component system, it was shown that the thermodynamics near gravothermal collapse is dominated by the the behavior of the heavy component (see in Ref. [19] discussions concerning asymptotic behavior (58) of gravothermal collapse temperature). Besides, the existence of mass-segregation due to the mass spectrum of constituents enables the occurrence of gravothermal collapse for energies higher than the ones associated to a system of identical particles. Accordingly, the presence of baryonic matter at the innermost regions of dark matter halos must trigger the formation of degenerate core of WDM particles via gravothermal collapse. Roughly speaking, this astrophysical phenomenon is quite similar to how the water condensation in atmosphere is triggered by the presence of condensation nuclei (e.g., dust particles). The formation of a degenerate core of WDM particles will provoke the reconcentration and the growth of velocity dispersions of baryonic matter trapped inside this region. Considering the empirical relations among the masses of supermassive black holes and the velocities dispersions σ of stars in the bulges of large galaxies [70–72], it is clear that the formation of a degenerate core of WDM particles favors the growth or even the formation of these exotic relativistic objects in galaxies with masses large enough.

The long-range character of gravitation ensures that the internal processes taking place in the galactic core disturb the whole system. In fact, the quantum-relativistic conditions governing the interior of galactic cores of large galaxies are driven by the overall masses of these stellar systems. Considering the quantum-relativistic mass bound (19), one obtains:

$$M_c \sim 6.4 \times 10^{12} M_\odot \tag{40}$$

for the case of WDM particle with mass $m = 2$ keV. Remarkably, this characteristic mass is comparable to the typical mass of large galaxies, e.g., the mass of our Milky way is $M = (0.8 - 1.5) \times 10^{12} M_\odot$ [73]. The present heuristic arguments suggest that the properties of the large galaxies could be explained by quantum-relativistic processes involving WDM particles (e.g., the formation of supermassive black hole via the relativistic gravothermal collapse of degenerate cores of WDM particles). In other words: *in the same way that the characteristic mass (20) explains the properties of stars in terms of baryonic matter, the characteristic mass (40) should explain the observed properties of large galaxies if DM halos are composed of WDM particles with mass m in the keV scale.*

Unfortunately, the analysis of the previous possibility is much beyond the reach of fermionic King model. It requires a relativistic approach analogous the one developed by Chavanis and Alberti in Refs. [41,74–76], but including the incidence of evaporation effects. In general, one could expected many qualitative behaviors similar to the ones reported in Refs. [41,74,76] replacing the box radius by the tidal radius. Accordingly, the relativistic approach of fermionic King model should be hallmarked by *three characteristic lengths*: the tidal radius R, the Fermi radius R_F given by Equation (24), and the *Schwarzschild radius* $R_S = GM/c^2$. These three characteristic lengths enable us to introduce two mass ratios:

$$\theta = \left(\frac{R_F}{R}\right)^3 = \frac{M_F}{M} \quad \text{and} \quad \chi = \left(\frac{R_F}{R_S}\right)^{3/4} \propto \frac{M_c}{M}, \tag{41}$$

where M_F is the Fermi mass (25), while M_c is the quantum-relativistic mass bound (19). The thermodynamics of a relativistic fermionic King model will depend on these two characteristic masses. While the usual (classical) King model is compatible with any value of the total mass M, the fermionic King model is not consistent for masses below the lower bound $M_3 \simeq \frac{1}{4} M_F$ even for large energies (classical limit). For large values mass

and energies, the thermodynamic of fermionic King model is also affected by quantum correlations (see caloric curves shown in the right panel of Figure 2). I think that similar restrictions should be observed when the total mass M approaches the quantum-relativistic bound, $M \sim M_c$. In particular, one should observed the formation of a black hole from the gravitational collapse of the degenerate core as discussed in Ref. [76]. Any case, the relativistic models of self-gravitating fermions under evaporation are of great interest in the searching of WDM candidates. In principle, these models would enable the derivation of *upper bounds* for the mass of WDM particles. The key question here is to clarify the overall conditions in which a degenerate core of WDM particles collapses to form a black hole, and then contrast these predictions with observational data of galaxies population without super-massive black holes [77].

4. Conclusions

In this work, I have reviewed different aspects about the thermodynamics of astrophysical systems that undergo the evaporation of their constituents. These antecedents were employed to revisit precedent studies by de Vega and co-workers concerning warm dark matter in galactic halos [31–33]. According to the present analysis and precedent studies by Chavanis and co-workers [23], the empirical Burkert profile (32) employed to fit dark matter halos distributions can be associated to astrophysical models with evaporation effects for low energies close to gravothermal collapse. Using the reported parameters of the dwarf galaxy Willman 1, the upper bound (35) for the mass ratio $\theta = M_F/M$ enable us to derive the lower bound $m \geq m_{\min} = 1.2$ keV for WDM particles. According to this estimation, most of galaxies are massive enough to undergo a violent gravothermal collapse that leads to the formation of a degenerate core of WDM particles. Heuristic arguments were presented in favor that the formation of suppermassive black holes in large galaxies could be explained by a relativistic gravothermal collapse of degenerate core of WDM particles with mass m in the keV scale. This picture is highly supported by recent studies by Chavanis and Alberti concerning the relativistic description of self-gravitating fermions enclosed into a box [41,74,76]. In any case, the keV scale seems to be very important to explain the observed properties of dwarfs and large galaxies.

Before end this section, let us refer to some open problems. The present study should be generalized to describe a more general influence of evaporation, the presence of a mass spectrum for constituents, as well as the relativistic corrections. As already discussed, the classical King model (23) is just the case $\gamma = 1$ of the γ-exponential models (1). A natural extension for fermionic King model (42) is the following:

$$f(\mathbf{r}, \mathbf{p}|\beta, \varepsilon_c, \gamma) = \frac{E(x, \gamma)}{\alpha + e^x} H[x], \tag{42}$$

where $x = \beta[\varepsilon_c - \varepsilon(\mathbf{r}, \mathbf{p})]$ and $E(x, s)$ the generalized exponential function (2). Interesting aspects to be studied for the the previous *fermionic γ-exponential models* are: (a) if the incidence of quantum effects disturbs the occurrence of the called *asymptotic gravothermal collapse* [19], and (b) to clarify the γ-dependence of the upper bound (35) for the mass ratio parameter $\theta = M_F/M$. The presence of a mass spectrum is achieved considering the methodology discussed in Refs. [19,38]. The relativistic approach requires the adaptation of the methodology of Alberti and Chavanis [41,74,76] for a system of self-gravitating fermions that undergo the existence of evaporation. An important antecedent for this task is the called relativistic Woolley model developed by Katz and Horwitz [78,79], which should be regarded the case $\gamma = 0$ of relativistic γ-exponential models. Although the previous ingredients will provide a more complete picture to about the thermodynamics of dark matter halos, their consideration will involve a great complexity in the associated calculations. As already commented, these relativistic models of fermions would enable the derivation of upper bounds for the mass of WDM particles through the study of galaxies population without super-massive black holes [77].

Institutional Review Board Statement: Not applicable.

Informed Consent Statement: Not applicable.

Data Availability Statement: Structure parameters of galaxies shown in Table 1 are the same reported by de Vega and co-workers in Ref. [31].

Conflicts of Interest: The author declare no conflict of interest.

Appendix A. Additional Notes

The present work differs in mathematical notations and treatments with the work of Chavanis et al in Ref. [24]. These authors defined the *degeneration parameter* μ_{Ch} as follows:

$$\mu_{Ch} = \frac{\eta_0}{A}, \tag{A1}$$

where $\eta_0 = gm^4/h^3$ ($g = 2s + 1$) and the normalization constant A is given by:

$$A = \eta_0 e^{-\beta\varepsilon_m - \alpha_{Ch}}. \tag{A2}$$

Here, ε_m denotes the truncation energy, namely, the escape energy at which the particles leave the system. The constant α_{Ch} is related to the Fermi energy as $\varepsilon_F = -\alpha_{Ch}/\beta$. Consequently, the degeneration parameter μ_{Ch} can be written as:

$$\mu_{Ch} = \frac{\eta_0}{A} \equiv e^{\beta(\varepsilon_m - \varepsilon_F)}. \tag{A3}$$

In the Section II.E of Ref. [24], these authors invoked a dimensional analysis to *estimate* the degeneration parameter μ_{Ch} using the *typical radius R* and the *typical mass M*, and they obtained the correspondence:

$$\mu_{Ch} \sim \mu_{Box} \sim \eta_0 G^{\frac{3}{2}} M^{\frac{1}{2}} R^{\frac{3}{2}}, \tag{A4}$$

which looks equivalent to the expression

$$\mu_{Ch} \sim 1/\theta^{1/2} \tag{A5}$$

considering the mass ratio parameter θ introduced in Equation (25).

The degeneration parameter (A3) employed by Chavanis and co-workers corresponds to the normalization constant α introduced in Equation (42), which is expressed in terms of the Fermi energy ε_F, the cutoff (escape) energy ε_c and the temperature parameter β as $\alpha = e^{\beta(\varepsilon_c - \varepsilon_F)}$. The *degeneration parameter* μ employed as integration parameter of the Poisson problem (27) and the Fermi-King integral (28) is the variable

$$\mu = \ln\alpha = \beta(\varepsilon_c - \varepsilon_F), \tag{A6}$$

which is related to the degeneration parameter μ_{Ch} employed by Chavanis et al as:

$$\mu \equiv \ln\mu_{Ch}. \tag{A7}$$

The expressions (A4) and (A5) do not apply for the case of fermionic King model: a given value of the degeneration μ *corresponds to different values of the mass ratio parameter* θ because of the dependence of this quantity on the system energy (or the integration parameter Φ_0). This very fact is clearly shown in the left panel of Figure 2. Equation (A4)

was obtained for the model of self-gravitating fermions enclosed into a box [8], but it cannot be extrapolate to the case of fermionic King model. This feature explains why the thermodynamics of fermionic King model at constant degeneration parameter μ differs from its thermodynamics at constant total mass M. The study by Chavanis and co-workers in Ref. [24] concerns to the thermodynamics *at constant degeneration parameter μ* only. The thermodynamics of fermionic King model at constant total mass M has been recently discussed by Velazquez and Espinoza-Soliz in Ref. [25] to clarify the role of the total mass M on the thermodynamic stability. In fact, this second study employs the most relevant variables of the thermodynamic description: the total energy U, the total mass M and tidal radius R (regarded here as a fixed parameter that is equivalent to fix the volume V of the system). Such a description was invoked to obtain a re-derivation of bounds for WDM particles presented in this paper. Further details about the existing difference between these two frameworks are discussed in this precedent paper.

References

1. Padmanabhan, T. Statistical mechanics of gravitating systems. *Phys. Rep.* **1990**, *188*, 285–362. [CrossRef]
2. Antonov, V.A. English translation in: Dynamics of Globular Clusters, IAU Symp. 113. *Vestn. Leningr. Gos. Univ.* **1962**, *7*, 135.
3. Lynden-Bell, D. Statistical mechanics of violent relaxation in stellar systems. *Mon. Not. R. Astron. Soc.* **1967**, *136*, 101–121. [CrossRef]
4. de Vega, H.J.; Sanchez, N.G. The statistical mechanics of the self-gravitating gas: Equation of state and fractal dimension. *Phys. Lett. B* **2000**, *490*, 180–186. [CrossRef]
5. de Vega, H.J.; Sanchez, N.G. Statistical mechanics of the self-gravitating gas: I. Thermodynamic limit and phase diagrams. *Nucl. Phys. B* **2002**, *625*, 409–459. [CrossRef]
6. de Vega, H.J.; Sanchez, N.G. Statistical mechanics of the self-gravitating gas: II. Local physical magnitudes and fractal structures. *Nucl. Phys. B* **2002**, *625*, 460–494. [CrossRef]
7. Katz, J. Thermodynamics and Self-Gravitating Systems. *Found. Phys.* **2003**, *33*, 223–269. [CrossRef]
8. Chavanis, P.H. Phase transitions in self-gravitating systems. *Int. J. Mod. Phys. B* **2006**, *20*, 3113–3198. [CrossRef]
9. Velazquez, L.; Guzman, F. Alternative model of the Antonov problem. *Phys. Rev. E* **2003**, *68*, 066116. [CrossRef]
10. Velazquez, L.; Garcia, S.G.; Guzman, F. Alternative model of the Antonov problem: Generalization with the presence of a mass spectrum. *Phys. Rev. E* **2009**, *79*, 011120. [CrossRef]
11. King, I.A. The structure of star clusters. I. an empirical density law. *Astron. J.* **1962**, *67* 471–485. [CrossRef]
12. King, I.A. The structure of star clusters. II. Steady-state velocity distributions. *Astron. J.* **1965**, *70*, 376–383. [CrossRef]
13. King, I.A. The structure of star clusters. III. Some simple dynamical models. *Astron. J.* **1966**, *71*, 64–75. [CrossRef]
14. King, I.A. The structure of star clusters. IV. Photoelectric surface photometry in nine globular clusters. *Astron. J.* **1966**, *71*, 276–282. [CrossRef]
15. Gomez-Leyton, Y.J.; Velazquez, L. Truncated γ-exponential models for tidal stellar systems. *J. Stat. Mech.* **2014**, *P04006*. [CrossRef]
16. Woolley, R.V.D.R. A study of the equilibrium of globular clusters. *Mon. Not. R. Astron. Soc.* **1954**, *114*, 191–209. [CrossRef]
17. Wilson, C.P. Dynamical models of elliptical galaxies. *Astron. J.* **1975**, *80*, 175–187. [CrossRef]
18. Katz, J. Stability limits for 'isothermal' cores in globular clusters. *Mon. Not. R. Astron. Soc.* **1980**, *190*, 497–507. [CrossRef]
19. Gomez-Leyton, Y.J.; Velazquez, L. Truncated γ-exponential models: Evaporation and mass-segregation effects in the bi-component system. *Mon. Not. R. Astron. Soc.* **2019**, *488* 362–380. [CrossRef]
20. Ruffini, R.; Stella, L. On semi-degenerate equilibrium configurations of a collisionless self-gravitating Fermi gas. *Astron. Astrophys.* **1983**, *119*, 35–41.
21. Chavanis, P.H. On the coarse-grained evolution of collisionless stellar systems. *Mon. Not. R. Astron. Soc.* **1998**, *300*, 981–991. [CrossRef]
22. Chavanis, P.H.; Lemou, M.; Mehats, F. The Fermionic King Model. *arXiv* **2014**, arXiv:1411.6154.
23. Chavanis, P.H.; Lemou, M.; Mehats, F. Models of dark matter halos based on statistical mechanics: The classical King model. *Phys. Rev. D* **2015**, *91*, 063531 [CrossRef]
24. Chavanis, P.H.; Lemou, M.; Mehats, F. Models of dark matter halos based on statistical mechanics: The fermionic King model. *Phys. Rev. D* **2015**, *92*, 123527 [CrossRef]
25. Velazquez, L.; Espinoza-Soliz, I. Fermionic King model: Critical masses resulting from the competition of quantum and evaporation effects. *J. Stat. Mech.* under review
26. Chandrasekhar, S. On Stars, Their Evolution and Their Stability (Nobel Lecture) *Angew. Chem. Int. Ed. Engl.* **1984**, *23*, 679–689. [CrossRef]
27. Chandrasekhar, S.; Milne, E.A. The Highly Collapsed Configurations of a Stellar Mass, *Mon. Not. R. Astron. Soc.* **1931**, *91*, 456–466; [CrossRef]
28. Chandrasekhar, S. The Highly Collapsed Configurations of a Stellar Mass (second paper). *Mon. Not. R. Astron. Soc.* **1935**, *95*, 207–225. [CrossRef]

29. Oppenheimer, J.R.; Volkoff, G. M., On Massive Neutron Cores. *Phys. Rev.* **1939**, *55*, 374–381. [CrossRef]

30. Tolman, R.C. Static Solutions of Einstein's Field Equations for Spheres of Fluid. *Phys. Rev.* **1939**, *55*, 364-373. [CrossRef]

31. Destri, C.; de Vega, H. J.; Sanchez, N. G. Quantum WDM fermions and gravitation determine the observed galaxy structures. *Astropart. Phys.* **2013**, *46*, 14–22. [CrossRef]

32. Destri, C.; de Vega, H.J.; Sanchez, N.G. Fermionic warm dark matter produces galaxy cores in the observed scales because of quantum mechanics. *New Astron.* **2013**, *22*, 39–50. [CrossRef]

33. de Vega, H.J.; Salucci, P.; Sanchez, N.G. Observational rotation curves and density profiles versus the Thomas–Fermi galaxy structure theory. *Mon. Not. R. Astron. Soc.* **2014**, *442*, 2717–2727. [CrossRef]

34. Davoust, E. Analytical models for spherical stellar systems. *Astron. Astrophys.* **1977**, *61*, 391–396.

35. Binney, J.; Tremaire, S. *Galactic Dynamics*; Princeton University Press: Princeton, NJ, USA, 1984.

36. Chandrasekhar, S. *Principles of Stellar Dynamics*; Dover: New York, NY, USA, 1960.

37. Plummer, H.C. On the problem of distribution in globular star clusters. *Mon. Not. R. Astron. Soc.* **1911**, *71*, 460–470. [CrossRef]

38. Gieles, M.; Zocchi, A. A family of lowered isothermal models. *Mon. Not. R. Astron. Soc.* **2015**, *454*, 576-–592. [CrossRef]

39. Velazquez, L. Remarks about the thermodynamics of astrophysical systems in mutual interaction and related notions. *J. Stat. Mech.* **2016**, *2016*, P033105. [CrossRef]

40. Hertel, P.; Thirring, W. Free energy of gravitating fermions. *Commun. Math. Phys.* **1971** *24*, 22–36. [CrossRef]

41. Alberti, G.; Chavanis, P.H. Caloric curves of self-gravitating fermions in general relativity. *Eur. Phys. J. B* **2020**, *93*, 208. [CrossRef]

42. Navarro, J.F.; Frenk, C.S.; White, S.D.M. The Structure of Cold Dark Matter Halos. *Astrophys. J.* **1996**, *462*, 563–575. [CrossRef]

43. de Martino, I.; Chakrabarty, S.S.; Cesare, V.; Gallo, A.; Ostorero, L.; Diaferio, A. Dark Matters on the Scale of Galaxies. *Universe* **2020**, *6*, 107. [CrossRef]

44. Persic, M.; Salucci, P.; Stel, F. The universal rotation curve of spiral galaxies—I. The dark matter connection. *Mon. Not. R. Astron. Soc.* **1996**, *281*, 27–47. [CrossRef]

45. Colín, P.; Valenzuela, O.; Avila-Reese, V. Substructure and halo density profiles in a Warm Dark Matter Cosmology. *Astrophys. J.* **2000**, *542*, 622–630. [CrossRef]

46. Sommer-Larsen, J.; Dolgov, A. Formation of Disk Galaxies: Warm Dark Matter and the Angular Momentum problem. *Astrophys. J.* **2001**, *551*, 608–623. [CrossRef]

47. Gao, L.; Theuns, T. Lighting the Universe with filaments. *Science* **2007**, *317*, 1527–1530. [CrossRef] [PubMed]

48. Tikhonov, A.V.; Gottlöber, S.; Yepes, G.; Hoffman, Y. The sizes of minivoids in the local Universe: An argument in favour of a warm dark matter model? *Mon. Not. R. Astron. Soc.* **2009**, *399*, 1611–1621. [CrossRef]

49. Zavala, J.; Jing, Y.P.; Faltenbacher, A.; Yepes, G.; Hoffman, Y.; Gottlöber, S.; Catinella, B. The velocity function in the local environment from λcdm and λwdm constrained simulations. *Astrophys. J.* **2009**, *700*, 1779–1793. [CrossRef]

50. Papastergis, E.; Martin, A.M.; Giovanelli, R.; Haynes, M.P. The velocity width function of galaxies from the 40% ALFALFA survey: Shedding light on the cold dark matter overabundance problem. *Astrophys. J.* **2011**, *739*, 38. [CrossRef]

51. Lovell, M.R.; Eke, V.; Frenk, C.S.; Gao, L.; Jenkins, A.; Theuns, T.; Wang, J.; White, S.D.M.; Boyarsky, A. Oleg Ruchayskiy The haloes of bright satellite galaxies in a warm dark matter universe. *Mon. Not. R. Astron. Soc.* **2012**, *420*, 2318-—2324. [CrossRef]

52. Adhikari, R.; Agostini, M.; Ky, N.A.; Araki, T.; Archidiacono, M.; Bahr, M.; Baur, J.; Behrens, J.; Bezrukov, F.; Dev, P.S.B.; et al. A White Paper on keV sterile neutrino Dark Matter. *JCAP* **2017**, *01*, 025. [CrossRef]

53. Walker, M.; Peñarrubia, J. A Method for Measuring (Slopes of) the Mass Profiles of Dwarf Spheroidal Galaxies. *Astrophys. J.* **2011**, *742*, 20. [CrossRef]

54. Salucci, P.; Lapi, A.; Tonini, C.; Gentile, G.; Yegorova, I.; Klein, U. The universal rotation curve of spiral galaxies—II. The dark matter distribution out to the virial radius. *Mon. Not. R. Astron. Soc.* **2007**, *378*, 41–47. [CrossRef]

55. de Vega, H.J.; Salucci, P.; Sanchez, N.G. The mass of the dark matter particle: Theory and galaxy observations. *New Astron.* **2012**, *17*, 653–666. [CrossRef]

56. Gilmore, G.; Wilkinson, M.I.; Wyse, R.F.; Kleyna, J.T.; Koch, A.; Evans, N.W.; Grebel, E.K. The Observed Properties of Dark Matter on Small Spatial Scales. *Astrophys. J.* **2007**, *663*, 948–959. [CrossRef]

57. Simon, J.D.; Geha, M. The Kinematics of the Ultra-faint Milky Way Satellites: Solving the Missing Satellite Problem. *Astrophys. J.* **2007**, *670*, 313–331. [CrossRef]

58. Simon, J.D.; Geha, M.; Minor, Q.E.; Martinez, G.D.; Kirby, E.N.; Bullock, J.S.; Kaplinghat, M.; Strigari, L.E.; Willman, B.; Choi, P.I.; et al. A Complete spectroscopy survey of the Milky Way satellite Segue 1: The Darkest galaxy. *Astrophys. J.* **2011**, *733*, 46. [CrossRef]

59. Wolf, J.; Martinez, G.D.; Bullock, J.S.; Kaplinghat, M.; Geha, M.; Muñoz, R.R.; Simon, J.D.; Avedo, F.F. Accurate masses for dispersion-supported galaxies. *Mon. Not. R. Astron. Soc.* **2010**, *406*, 1220–1237. [CrossRef]

60. Brodie, J.P.; Romanowsky, A.J.; Strader, J.; Forbes, D.A. The Relationships among Compact Stellar Systems: A Fresh View of Ultracompact Dwarfs. *Astron. J.* **2011**, *142*, 199. [CrossRef]

61. Willman, B.; Strader, J. Galaxy, Defined. *Astron. J.* **2012**, *76*, 144. [CrossRef]

62. Martinez, G.D.; Minor, Q.E.; Bullock, J.; Kaplinghat, M.; Simon, J.D.; Geha, M. A Complete Spectroscopic Survey of the Milky Way satellite Segue 1: Dark matter content, stellar membership and binary properties from a Bayesian analysis. *Astrophys. J.* **2011**, *738*, 55. [CrossRef]

63. Bilic, N.; Munyaneza, F.; Tupper, G.B.; Viollier, R. D. The dynamics of stars near Sgr A* and dark matter at the center and in the halo of the galaxy. *Prog. Part. Nucl. Phys.* **2002**, *48*, 291–300. [CrossRef]

64. Bilic, N.; Tupper, G.B.; Viollier, R.D. Dark Matter in the Galaxy. In *Particle Physics in the New Millennium, Lecture Notes on Physics 616*; Springer: Berlin/Heidelberg, Germany, 2003; pp. 24–38.

65. Bilic, N.; Viollier, R.D. Dark Matter Concentration in the Galactic Center. *Phys. Lett. B* **1997**, *408*, 75.

66. Tsiklauri, D.; Viollier, R.D. Dark Matter Concentration in the Galactic Center. *Astrophys. J.* **1998**, *500*, 591. [CrossRef]

67. Bilic, N.; Viollier, R.D. Gravitational phase transition of fermionic matter in a general-relativistic framework. *Eur. Phys. J. C* **1999**, *11*, 173–180. [CrossRef]

68. Bilic, N.; Viollier, R.D. General relativistic Thomas-Fermi model. *Gen. Rel. Grav.* **1999**, *31*, 1105–1113. [CrossRef]

69. Bilic, N.; Lindebaum, R.J.; Tupper, G.B.; Viollier, R.D. On the formation of degenerate heavy neutrino stars. *Phys. Lett. B* **2001**, *515*, 105–110. [CrossRef]

70. Marconi, A.; Hunt, L. The Relation between Black Hole Mass, Bulge Mass, and Near-Infrared Luminosity. *Astrophys. J.* **2003**, *589*, L21–L24. [CrossRef]

71. Ferrarese, L.; Merritt, D. A Fundamental Relation between Supermassive Black Holes and Their Host Galaxies. *Astrophys. J.* **2000**, *539*, L9–L12. [CrossRef]

72. Gebhardt, K.; Bender, R.; Bower, G.; Dressler, A.; Faber, S.M.; Filippenko, A.V.; Green, R.; Grillmair, C.; Ho, L.C.; Kormendy, J.; et al. A Relationship between Nuclear Black Hole Mass and Galaxy Velocity Dispersion. *Astrophys. J.* **2000**, *539*, 13. [CrossRef]

73. McMillan, P.J. The mass distribution and gravitational potential of the Milky Way. *Mon. Not. R. Astron. Soc.* **2017**, *465*, 76—94. [CrossRef]

74. Chavanis, P.H. Statistical mechanics of self-gravitating systems in general relativity: I. The quantum Fermi gas. *Eur. Phys. J. Plus* **2020**, *135*, 290. [CrossRef]

75. Alberti, G.; Chavanis, P.H. Caloric curves of classical self-gravitating systems in general relativity. *Phys. Rev. E* **2020**, *101*, 052105. [CrossRef] [PubMed]

76. Alberti, G.; Chavanis, P.H. Gravitational phase transitions and instabilities of self-gravitating fermions in general relativity. *Phys. Lett. B* **2020**, *801*, 135155.

77. Gebhardt, K.; Lauer, T.R.; Kormendy, J.; Pinkney, J.; Bower, G.A.; Green, R.; Gull, T.; Hutchings, J.B.; Kaiser, M.E.; Nelson, C.H.; et al. M33: A Galaxy with No Supermassive Black Hole. *Astron. J.* **2001**, *122*, 2469–2476. [CrossRef]

78. Katz, J.; Horwitz, G. Thermodynamic stability of relativistic rotating stellar configurations and a maximum principle for the entropy. *Astrophys. J.* **1974**, *194*, 439–449. [CrossRef]

79. Katz, J.; Horwitz, G. Steepest descent technique and stellar equilibrium statistical mechanics. II—Relativistic clusters in a box. *Astrophys. J. Suppl. Ser.* **1977**, *33*, 251–268. [CrossRef]